Mullite and Mullite/ZrO$_2$-7wt.%Y$_2$O$_3$ Powders for Thermal Spraying of Environmental Barrier Coatings

E. Garcia, J. Mesquita-Guimarães, P. Miranzo, M.I. Osendi, Y. Wang, R.S. Lima, and C. Moreau

Mullite and mullite/ZrO$_2$-7wt.%Y$_2$O$_3$ coatings could be thought among the main protective layers for environment barrier coatings (EBCs) to protect Si-based substrates in future gas turbine engines. Considering that feedstock of the compound powder is not commercially available, two powder processing routes Spray Drying (SD) and Flame Spheroidization (FS) were implemented for both types of powders. For each method the particle size, the morphology, and microstructure of the powder particles was determined. In addition, the effect of the heat treatment on the powder crystallinity and microstructure of FS powders was also investigated. To evaluate their suitability as feedstock materials, the powders were plasma sprayed and their in-flight particle characteristics monitored for coatings production. The powder morphology was correlated to the in-flight particle characteristics and splat morphology to gain insight about into the influence of powder characteristics on the coating formation.

1. Introduction

Mullite has been considered as a transitional protective layer for Si-based ceramics (Si$_3$N$_4$, SiC) components to be used in future gas turbines (Ref 1, 2). The functionality of this layer is to inhibit substrate corrosion by water vapor whereas taking advantage of its close thermal expansion coefficient to those of non-oxide ceramics (Ref 1, 3). One of the main drawbacks of plasma-sprayed mullite coatings is that an important amount of amorphous phase develops, which may cause coating spall-off when thermal cycled (Ref 4, 5). It was also found that even fully crystalline

E. Garcia, J. Mesquita-Guimarães, P. Miranzo, and **M.I. Osendi,** Institute of Ceramics and Glass, CSIC, C/Kelsen 5, Campus de Cantoblanco, 28049 Madrid, Spain; and **Y. Wang, R.S. Lima,** and **C. Moreau**, National Research Council of Canada (NRC), Boucherville, QC, Canada. Contact e-mail: Garcia@icv.csic.es

mullite coatings exhibited volatilization of silica in water steam atmospheres (Ref 6, 7). To solve these problems different approaches have been attempted during the last years. The first attempt was to plasma spray ZrO$_2$-7-8 wt.% Y$_2$O$_3$ (YSZ) as a top coat on the mullite layer to improve the lifetime of the ceramic component (Ref 8). In this case, the large coefficient of thermal expansion (CTE) mismatch between YSZ and mullite coatings caused the failure of the system. Next, a new three layer system was developed based on a top coat of BaO-SrO-Al$_2$O$_3$-SiO$_2$ (BSAS), a crack resistant mullite plus BSAS intermediate layer, and finally, a silicon bond coat (Ref 9). Other approach suggested replacing the BSAS top coat with rare earth monosilicates due to their phase stability and closer CTE to silicon-based ceramic substrates (Ref 10) and, in particular, the use of Lu$_2$Si$_2$O$_7$ disilicates or the Lu$_2$Si$_2$O$_7$/mullite eutectic mixture (Ref 1). The major concern with these multilayered systems was the development of through-thickness cracking in the coating. Other studies, focused on adding a low thermal conductivity thermal layer like the YSZ, on top of the BSAS-based EBCs (Ref 11). The so-called thermal-environmental barrier coating (TEBC) system was formed by five layers where a transition layer between YSZ and BSAS or mullite coating was required to gradually adjust their CTE mismatches. Furthermore, Withey et al. (Ref 12) showed that an YSZ/mullite (46 vol.%/54 vol.%) free-standing plasma sprayed coating showed enhanced creep resistance than a YSZ alone coating and may be used as a thermal barrier coating. Nonetheless, they prepared this coating by mixing two commercial sprayable powders as the composition was not commercially available.

Therefore, preparing mullite/ZrO$_2$ granules from fine powders that can be suitable for plasma spraying was the main aim of present work. In this work, mullite as well as

an equally by volume mulite/ZrO$_2$ mixture have been prepared. The agglomerated powders were obtained by spray drying water suspensions of the original fine powders after controlling their stability with surfactants. Spray drying is an economical and continuous operation which can produce uniform and reliable powders. Temperature, binders, pressure, and atomization system are only a few parameters to mention, together with the characteristics of the suspension (Ref 13) that can affect the morphology and size of the agglomerates. The spherical morphology required for an even flow of the particles through the plasma torch can be achieved in this way (Ref 14). Furthermore, the spray-dried powders should exhibit cohesive strength levels to withstand the turbulence of the spray jet without breaking apart and a proper size distribution. If the spray-dried powders are too fine and porous (low cohesive strength) they do not exhibit enough inertia required to cross the streamlines of the spray jet, being projected to its periphery without depositing on the substrate. They may also evaporate by superheating before splashing on the substrate, resulting in a poor deposition efficiency and weak bonding (Ref 15). To increase powder density, these spray-dried batches were flame sprayed into a water container to get higher spheroidization and compactness of the particles. This technique has been employed previously to get solid spheres in the micron range of different ceramic and glass ceramic compositions (Ref 16).

By changing plasma spraying parameters and/or powders characteristics, control over speed and temperature of the particles can be achieved and variations in the crystallization degree are seen (Ref 17). Therefore, characteristics of the feeding powders, such as size, shape, and density can play a main role and deserve attention. Finally, preliminary results over the in-flight properties of the single splats, their aspect once impacted on a SiC substrate and the coatings built-up are presented for the mullite powders prepared under different conditions.

2. Experimental

Commercial powders of mullite (3Al$_2$O$_3$·2SiO$_2$) and zirconia, stabilized with 7 wt.% Y$_2$O$_3$ (Y-TZP), were used. Mullite powders (Baikalox SASM, Baikowski Chemie, Annecy, France) have a purity of 99% and an average particle size of 1.3 μm. Y-TZP powders (TZ4Y, Tosoh, Tokyo, Japan) were 99.95% pure with a composition of 93 wt.% ZrO$_2$-7.0 wt.% Y$_2$O$_3$ and an average particle size of 0.3 μm. Two different water suspensions, mullite and the 50 vol.%mullite-50 vol.%Y-TZP named mullite/ZrO$_2$, both with a 30 wt.% of solid content, were prepared. To condition the suspensions, 0.4 wt.% of a polyelectrolyte dispersant (Dolapix CE 64 CA, Zschimmer-Schwarz, Lahnstein, Germany) and 5 wt.% of a polysaccharide binder (KB 1247, Zschimmer-Schwarz, Lahnstein, Germany) were added. The thorough mixing of all ingredients was assured by using a blade mixer and,

subsequently, a continuous attrition mill to avoid powders agglomeration. Due to their nature, none of the additives left residues after high temperature exposure.

The slurries were spray-dried with a rotary atomizer spray drying system (Mobile Minor Spray Dryer, basic model, Niro Atomizer, Søborg, Denmark) in a co-current flow. The inlet temperature ranged from 300 to 350 °C and that at exit of the spray dryer from 100 to 150 °C. The slurry was fed at 65 mL/min and 3 × 10^5 Pa of air pressure. For the Flame Spheroidization (FS) method, corresponding batches of spray dried powders were sprayed into a water filled metal container using an oxygen-acetylene gun (model CastoDyn DS 8000, Eutectic Castolin, Madrid, Spain), at the stand-off distance of 15 cm. Afterwards, water was evaporated at 120 °C and FS powders were heat treated in a furnace at 1300 °C for 1 h.

Particle size distributions of the SD and heat-treated FS powders were determined with a laser diffraction analyzer (Mastersizer S, Malvern, UK). The microstructure of the different particles was viewed with a scanning electron microscope (SEM) (DMS-950 Carl-Zeiss, Germany) and x-ray energy dispersive spectroscopy (EDS), elemental mapping for Al (K), Si (K), and Zr (L) were also done in the granules. X-ray diffraction analyses (XRD) were performed using a Xpert PRO difractometer (PANalytical, Netherlands) with a θ/2θ configuration, in the 10-70 2θ range, with a step of 0.0165°, a time per step of 50 s and 15 rpm of sample spinning, in order to track the amorphization and subsequent crystallization of powders after the thermal treatment of the FS batches. A commercially available mullite fused and crushed (FC) powder (Mullite #1020, Saint-Gobain, Worcester, MA, USA) was used as a benchmark material. Finally, the three mullite powders (SD, FS, FC) were thermally sprayed (APS) with an air plasma spray torch (Axial III, Northwest Mettech, North Vancouver, BC, Canada) on as-received SiC substrates (Hexoloy SA, Saint-Gobain,
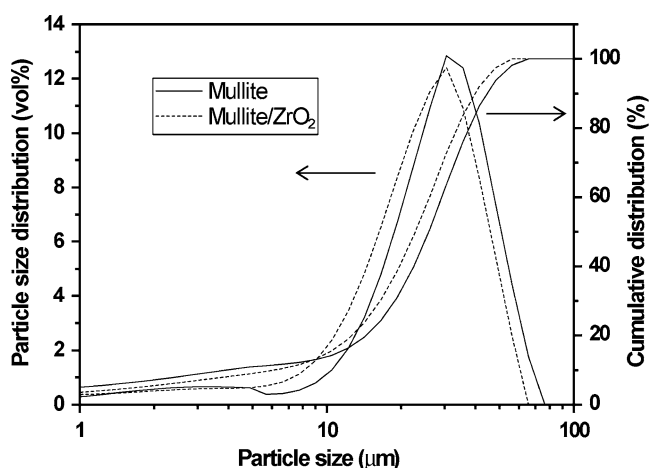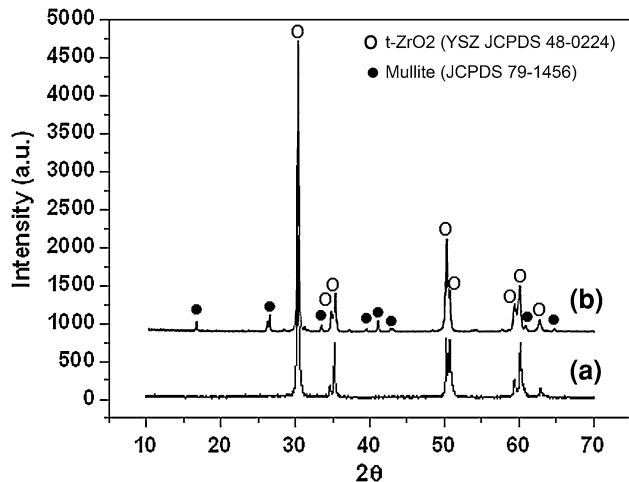

Fig. 1 Particle size distributions for SD mullite (*solid line*) and mullite/ZrO$_2$ powders (*dashed line*)
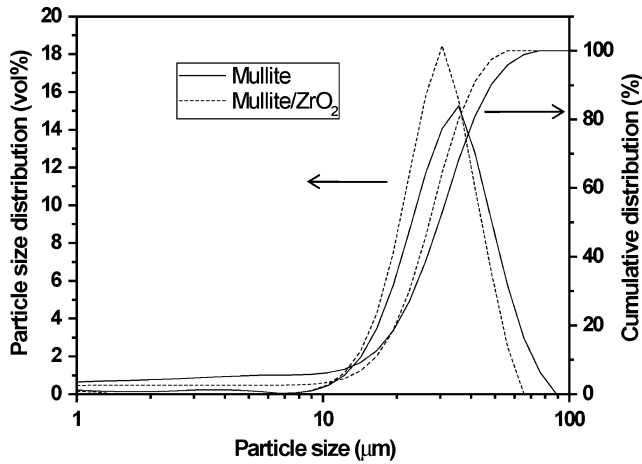
Fig. 2 Particle size distributions for FS mullite (*solid line*) and mullite/ZrO$_2$ powders (*dashed line*)
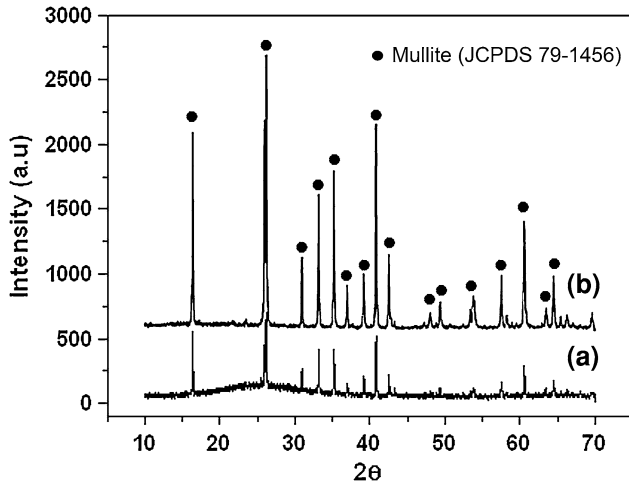
Fig. 3 XRD patterns for FS mullite powders (a) and after heat treatment (b) showing peak adscription


**Fig. 4** XRD patterns for FS mullite/ZrO$_2$ powders (a) and after heat treatment (b) showing peak adscription

Worcester, MA, USA). SEM microstructure of splat collected and coatings deposited on those substrates are presented. The temperature (T) and velocity (V) of the particles were determined in-flight using a commercially available diagnostic system DPV-2000 (Tecnar Automation, St-Bruno, QC, Canada).

3. Results and Discussion

The average particle sizes (d_{50}) of the SD powders of mullite and mullite/ZrO$_2$ were 26 and 23 μm, respectively. In Fig. 1, the particle size distributions for both powders are depicted, both are very similar extending over the
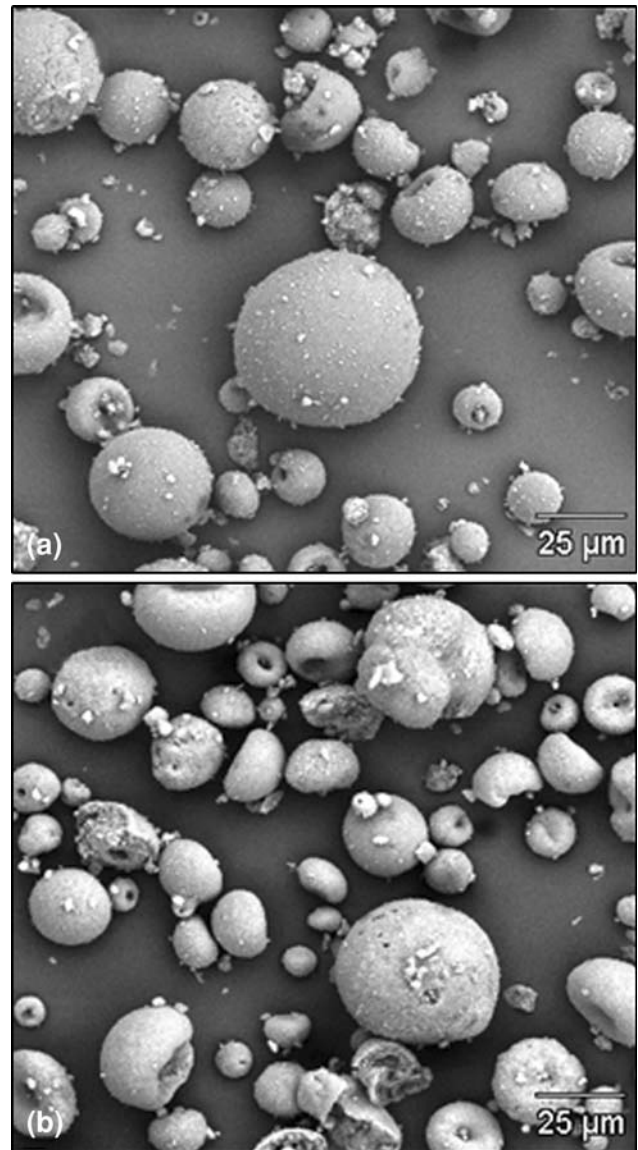
Fig. 5 SEM micrographs of SD (a) mullite powders and (b) mullite/ZrO$_2$ powders
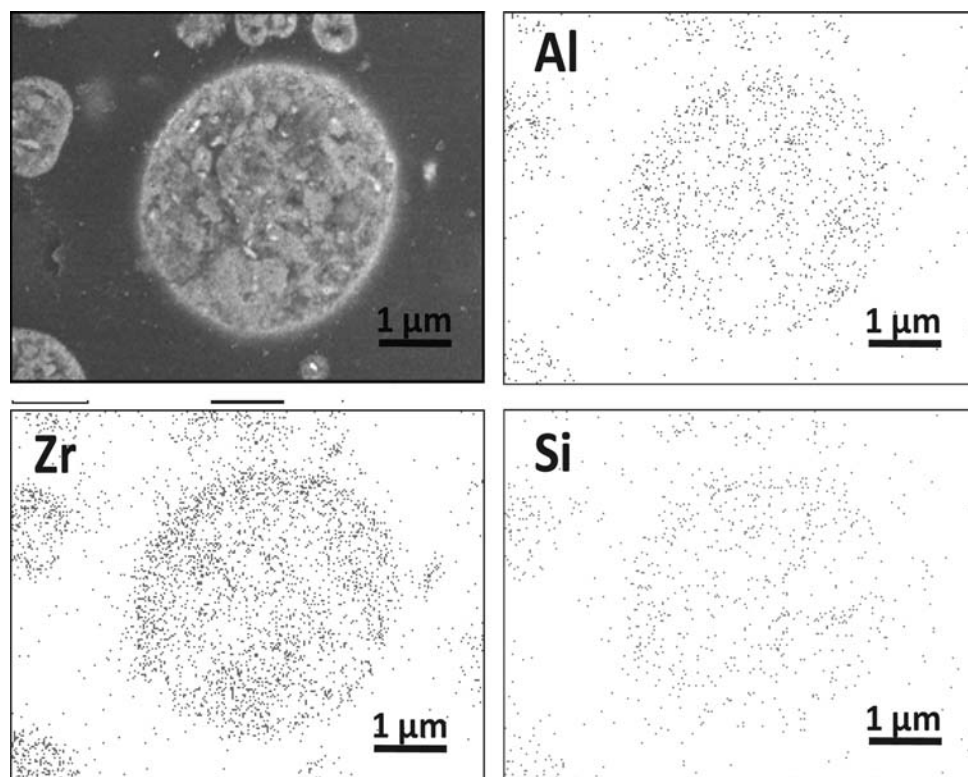
Fig. 6 SEM micrographs of a SD mullite granule with corresponding elemental mapping of Al, Si, and Zr

range 1 to 70 μm. For the corresponding FS batches, a slight increase in d_{50} is detected, 30 μm for mullite and 27 μm for mullite/ZrO_2 and narrower distributions are observed, as shown in Fig. 2. This increase in the average size can be attributed to the preferential vaporization of smaller particles during the FS process.

In Fig. 3(a), XRD pattern for the FS mullite powder shows a hump around 25° (2θ) with characteristics mullite peaks over imposed. Depending on the intimate level of atomic mixing, the crystallization of mullite for a Al_2O_3/SiO_2 mixture can take place around 1000 °C or else a further thermal increase to temperatures ~1280 °C may be required (Ref 18, 19). Therefore, after treating at 1300 °C the FS powders, sharp and intense XRD peaks of mullite are observed (Fig. 3b). Therefore, the FS process produced amorphization of the SD mullite powders, which recover full crystallinity after the heat treatment.

In a similar way, the mullite/ZrO_2 mixture exhibits the same effect regarding crystallization of mullite as it is seen in Fig. 4, where XRD patterns before and after the heat treatment are depicted. The tetragonal phase of ZrO_2 is detected in the XRD patterns of the FS powders, although its intensity increases after the thermal treatment. Therefore, the injection of both constituents (mullite + YSZ) in the plasma torch does not produce destabilization of the YSZ. Similarly, the t-ZrO_2 phase was the main ZrO_2 phase in flame-sprayed mullite/ZrO_2 coatings when using

mullite and pure monoclinic ZrO_2 powders (Ref 20) as feedstock material.

SEM micrographs of the SD powders are shown in Fig. 5, where mainly rounded soft particles are observed. When granules appeared broken their inside porous structure is seen. Both mullite and mullite/ZrO_2 SD powders have similar features. To verify the homogeneity of the mullite/ZrO_2 mixture after the SD process, some granules were immersed in epoxy resin under vacuum, ground and polished for microstructural analysis. EDS mappings for the Zr, Al, and Si elements of a granule cross section are shown in Fig. 6, where clear zones correspond to the ZrO_2 phase and gray areas to the mullite phase, both homogenously mixed within the granules. Therefore, during the SD process no segregation of both phases occurred in spite of the differences in particle size and density of both constituents.

On the other hand, the FS powders were spheres of compacted granules (Fig. 7). In the case of mullite, surfaces look smooth (Fig. 7a), whereas some mullite/ZrO_2 particles show crystallization at their surface (Fig. 7c). When particles are sectioned and polished, the essentially solid nature of these granules is evidenced (Fig. 7b, d). Therefore, the SD granules seem to sinter during the FS process, although the d_{50} remains quite similar to the original SD powders. Furthermore, fewer smaller granules are detected (Fig. 7), which also supports the assumed vaporization of tiny particles during flame spraying.
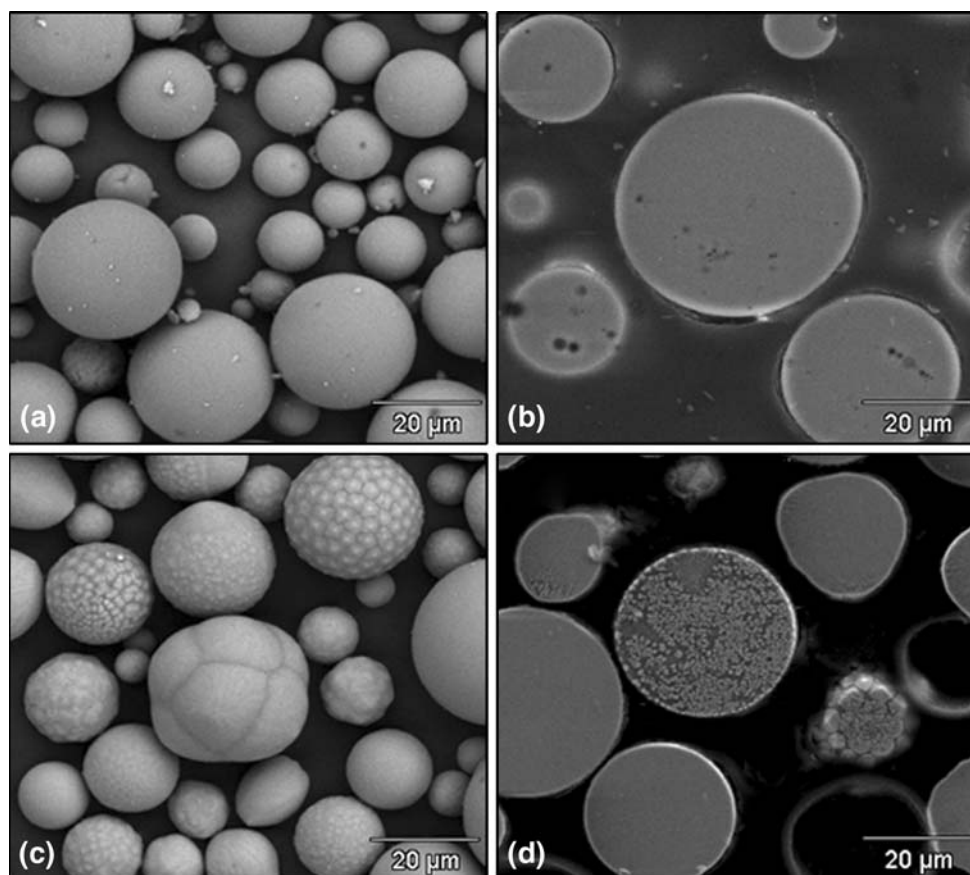
Fig. 7 SEM micrographs of FS mullite powders, (a) surface view (b) polished cross section and mullite/ZrO_2 powders (a) surface view (b) polished cross section

The structure observed in the FS mullite/ZrO_2 powders is enhanced after the treatment, as it can be observed in Fig. 8, where details of surface (Fig. 8b) and polished cross section reveal extensive crystallizations (Fig. 8c). The dendritic morphology of these crystals (Ref 21, 22) and the XRD results indicate that they correspond to the t-ZrO_2 phase (Fig. 4).

To analyze the viability of these different powders for plasma spraying, the mullite powders were sprayed using the spray parameters of Table 1, chosen for coating production. The temperature (T) and velocity (V) of these particles were monitored. In addition, some in-flight particles were also collected on SiC substrates in order to analyze the splat morphology. All particle T and V values were measured at the spray distance of 10 cm. Results for the commercial FC mullite powder, are also included. It is evidenced that with the SD powders the coatings were obtained with spraying conditions exhibiting the highest velocities (760 m/s) and the lowest temperatures. This behavior can be explained by its porous nature compared to those of the other two powders (Fig. 5). Table 1 shows that the FS and FC powders were sprayed using the 1.27 cm diameter nozzle of the Axial III torch, whereas, the SD one was sprayed using a narrower nozzle (0.8 cm).

The velocity of a gas passing through a nozzle is proportional to its flow rate (Fr) over the nozzle diameter (d) ratio, i.e., Fr/d. As all particles were sprayed at the same total gas flow rate (Table 1), the narrower nozzle employed to spray the SD particles may have impinged higher velocities to these particles. However, the compositions of the plasma gases also have to be taken into account. For example, the SD particles were sprayed by using Ar-based plasma, whereas, the other particles were sprayed via a richer N_2-based plasma. Ar-based plasmas induce higher particle velocities and lower particle temperature levels than those with a high N_2 content (Ref 23). Between the dense FS and commercial mullite powders, differences in V are lower and the higher velocity of the FS powders can be attributed to their better flow inside the plasma jet associated to their spherical shape.

Single splats collected on SiC substrates and the coatings obtained are compared in Fig. 9 for the SD, FS, and FC powders. The splats were collected by performing one single torch pass (forming a spray bead) at 60 cm/s over the SiC substrates that were at room temperature and at the spray distance of 10 cm. SD powders formed splats of irregular shape with a rough core
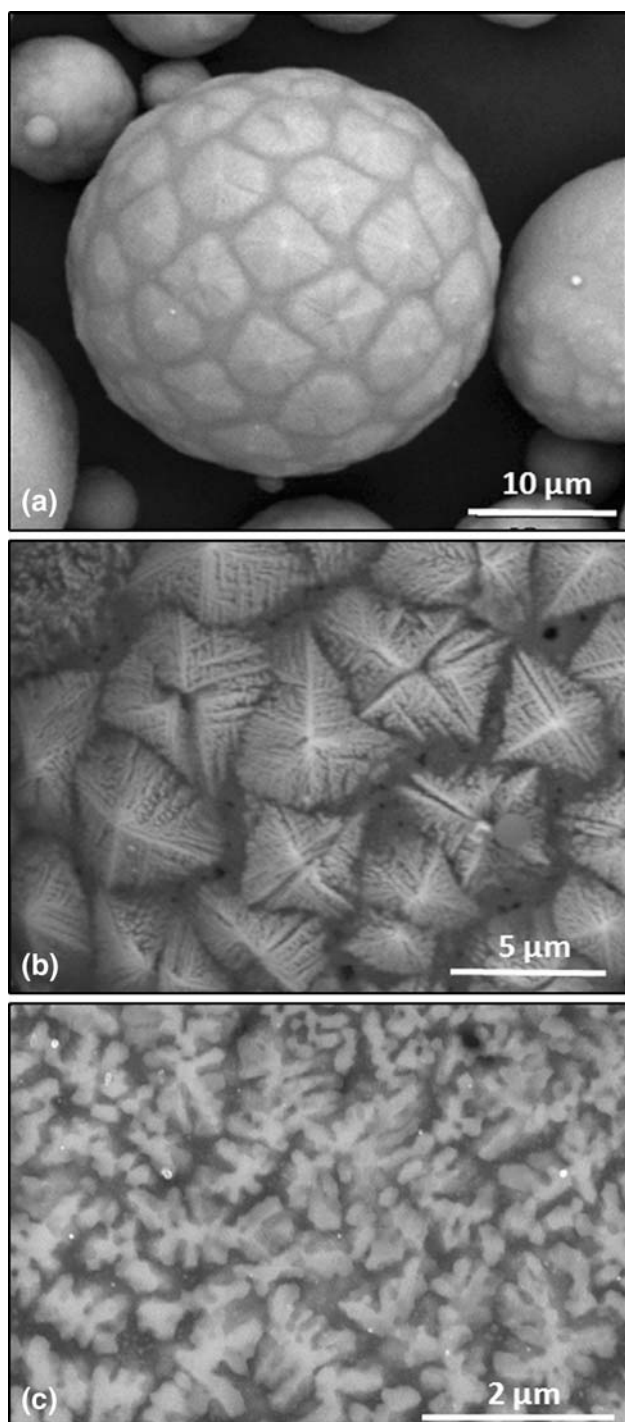
Fig. 8 SEM micrographs showing detail of FS mullite/ZrO$_2$ granule after heat treatment (a), (b) surface view, and (c) polished cross section

surrounded by a molten shell, especially for larger splats (Fig. 9a.1). This observation agrees with the high in-flight speed of the granules and their porous quality, which

reduces heat transfer inside the granule. The smaller size splats look completely melted. In Fig. 9(a.2) a detail of the coatings obtained with this powder is shown, which, as expected from the analysis of the splat collection, is a built-up of both molten and un-melted particles. This can benefit the coating crystallinity if correct adherence of the splats is provided. Regarding the FS powders (Fig. 9b.1), splats appear melted but not all of them are fully flattened, in addition, some entrapped porosity in the flattened zone is seen. This situation is clearly seen in the corresponding coating of Fig. 9(b.2), which is formed by a mixture of molten particles and spherical features related with the un-melted FS feedstock. For FC powders, less melted splats are seen for a similar scanned zone (Fig. 9c.1). Entrapped porosity is also detected in this case when analyzing the corresponding coating (Fig. 9c.2). Comparing splats and coatings for FS and FC, both having dense granules, the differences in the flattening appearance are attributable to differences in morphology. The spherical shape of the FS unmelted particles is easier to distinguish within the coating that the blocky shaped FC particle. A comparative study of the coating properties obtained with these powders has been published elsewhere (Ref 17), showing that dense particles (e.g., FS) can be used to engineer highly crystalline coatings, whereas, SD powders are suitable to tailor coatings that exhibit high crystallinity-to-elastic modulus ratios.

Mullite and mullite/ZrO$_2$ mixtures agglomerated by SD and FS methods are adequate feedstock powders for plasma spraying techniques with spraying behavior similar to mullite standard commercial powders. Powders of same composition and size but with different degree of crystallinity and density can be processed (SD, FS) to achieve particular coating conditions.

4. Conclusions

Agglomerated mullite and mullite/ZrO$_2$ (50/50 vol.%) compositions exhibiting different characteristics have been processed using spray drying and flame spraying spheroidization. Both types of granules presented similar sizes, although spheroidization process narrowed the size distribution due to the vaporization of the lower sized granules. Both, in-flight particle temperatures and velocities depended on the characteristics of the granules; SD granules were porous and then reached the substrate at lower temperatures and higher velocities, compared to fused and crushed mullite particles, developing splats of irregular shape. On the other hand, FS granules were denser achieving in-flight temperatures and velocities similar to those of FC. Mullite granules became amorphous after the FS process whereas mullite/ZrO$_2$ granules still showed t-ZrO$_2$ phase. Re-crystallization of mullite was reversible by heat treatment at 1300 °C.

Table 1 Spraying parameters used for the mullite powders and in-flight particles data (DPV-2000 system)

Powder	Gas flow, slpm	Feed rate, g/m	Plasma Gas (%)			Ø Nozzle	T, ºC	V, m/s
			Ar	N_2	H_2			
Mullite SD	280	10	80	10	10	0.8 cm (5/16″)	2120 ± 321	760 ± 117
Mullite FS			45	45	10	1.27 cm (1/2″)	2622 ± 212	566 ± 79
Mullite 1020* (FC)			45	45	10		2601 ± 175	442 ± 62

The spray distance was 10 cm for all the conditions
* Saint Gobain, Worcester, MA, USA
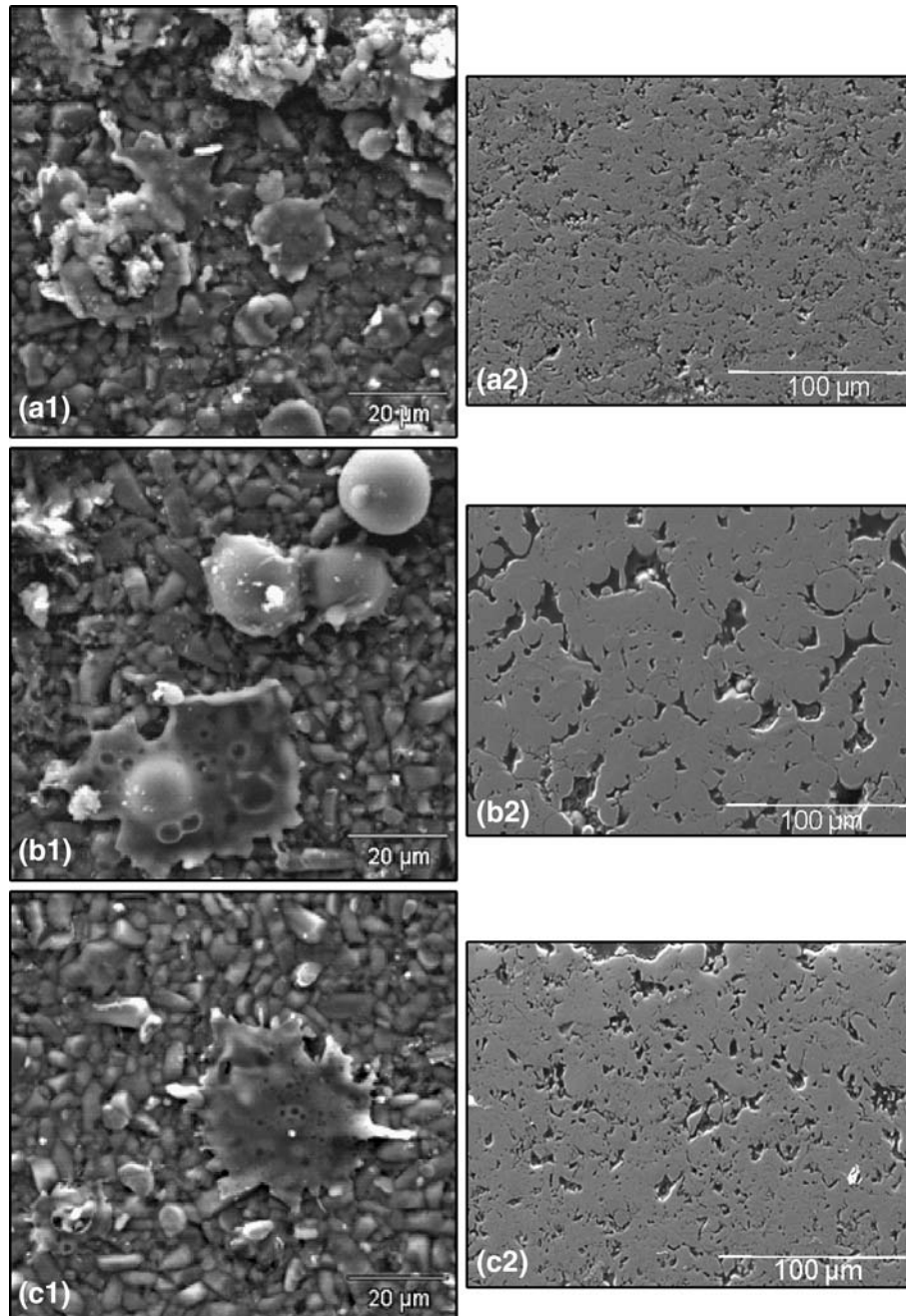
Fig. 9 SEM micrographs of individual splats and coatings deposited on SiC substrates of: SD powders (a), FS powders (b), and fused and crushed commercial powders (c), all with mullite composition
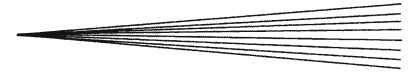
References

1. S. Ueno, D.D. Jayaseelan, and T. Ohji, Development of Oxide-Based EBC for Silicon Nitride, *Int. J. Appl. Ceram. Technol.*, 2004, **1**(10), p 362-373
2. N. Miriyala, J. Kimmei, J. Price, K. More, P. Tortorelli, H. Eaton, G. Linsey, and E. Sun, The Evaluation of CFCC Liners after Field Testing in a Gas Turbine—III, *Proceedings of ASME TURBO EXPO 2002*, June 3-6, 2002 (Amsterdam, The Netherlands), ASME, 2002, p 1-10
3. R. Krishnamurthy, B.W. Sheldon, and J.A. Haynes, Stability of Mullite Protective Coatings for Silicon-Based Ceramics, *J. Am. Ceram. Soc.*, 2005, **88**(5), p 1099-1107
4. S. Ueno, T. Ohji, and H.-T. Lin, Corrosion and Recession of Mullite in Water Vapor Environment, *J. Eur. Ceram. Soc.*, 2008, **28**, p 431-435
5. K.N. Lee, Current Status of Environmental Barrier Coatings for Si-Based Ceramics, *Surf. Coat. Technol.*, 2000, **33-34**, p 1-7
6. K.N. Lee, R.A. Miller, N.S. Jacobson, and S. Nathan, New Generation of Plasma-Sprayed Mullite Coatings on Silicon Carbide, *J. Am. Ceram. Soc.*, 1995, **78**, p 705-710
7. K.N. Lee and R.A. Miller, Oxidation Behavior of Mullite-Coated SiC and SiC/SiC Composites under Thermal Cycling Between Room Temperature and 1200°-1400 °C, *J. Am. Ceram. Soc.*, 1996, **79**, p 620-626
8. K.N. Lee, D.S. Fox, J.I. Eldrige, D. Zhu, R.C. Robinson, N.P. Bansal, and R.A. Miller, Upper Temperature Limit of Environmental Barrier Coatings Based on Mullite and BSAS, *J. Am. Ceram. Soc.*, 2003, **86**, p 1299-1306
9. K.L. More, P.F. Tortorelli, L.R. Walter, J.B. Kimmel, N. Miriyala, J.R. Price, E.Y. Sun, and G.D. Linsey, Evaluating Environmental Barrier Coatings on Ceramic Matrix Composites After Engine and Laboratory Exposures, ASME paper 2002-GT-30630, IGTI 4 A, p 155-162
10. K.N. Lee, D.S. Fox, and N.P. Bansal, Rare Earth Silicate Environmental Barrier Coatings for SiC/SiC Composites and Si₃N₄ Ceramics, *J. Eur. Ceram. Soc.*, 2005, **25**, p 1705-1715
11. I. Spitsberg and J. Steibel, Thermal and Environmental Barrier Coatings for SiC/SiC CMCs in Aircraft Engine Applications, *Int. J. Appl. Ceram. Technol.*, 2004, **1**, p 291-301
12. E. Withey, C. Peorak, R. Trice, G. Dickinson, and T. Taylor, Design of 7 wt% Y_2O_3-ZrO_2/Mullite Plasma Sprayed Composite Coatings for Increased Creep Resistance, *J. Eur. Ceram. Soc.*, 2007, **27**, p 4675-4683
13. G. Bertrand, P. Roy, C. Filiatre, and C. Coddet, Spray-dried Ceramic Powders: A Quantitative Correlation Between Slurry Characteristics and Shapes of the Granules, *Chem. Eng. Sci.*, 2005, **60**, p 95-102
14. V. Viswanathan, K.E. Rea, A. Vaidya, and S. Sealw, Role of Spray Drying of Nanoagglomerates in Morphology Evolution in Nanostructured APS Coatings, *J. Am. Ceram. Soc.*, 2008, **91**(2), p 379-386
15. X.Q. Cao, R. Vassen, S. Schwartz, W. Jungen, F. Tietz, and D. Stöever, Spray-Drying of Ceramics for Plasma-Spray Coating, *J. Eur. Ceram. Soc.*, 2000, **20**, p 2433-2439
16. A. Rosenflanz, M. Frey, B. Endres, T. Anderson, E. Richards, and C. Schardt, Bulk Glasses and Ultrahard Nanoceramics Based on Alumina and Rare-earth Oxides, *Nature*, 2004, **430**, p 761-764
17. Y. Wang, R.S. Lima, C. Moreau, E. Garcia, J. Guimaraes, P. Miranzo, and M.I. Osendi, Mullite Coatings Produced by APS and SPS: Effect of Mullite Powder Morphology and Spray Processing on the Microstructure, Crystallinity and Mechanical Properties, *Proceedings of ITSC 2009: Expanding Thermal Spray Performance to New Markets and Applications*, B.R. Marple, M.M. Hyland, Y.-C. Lau, C.-J. Li, R.S. Lima, and G. Montavon, Ed., Pub. ASM International, Materials Park, OH, USA, 2009 (CD-ROM)
18. K. Srikrishna, G. Thomas, R. Martinez, M.P. Corral, S. De Aza, and J.S. Moya, Kaolinite-Mullite Reaction Series: A TEM Study, *J. Mater. Sci.*, 1990, **25**, p 607-612
19. E. Tkalcec, S. Kurajica, and H. Ivankovic, Diphasic Aluminosilicate Gels with Two Stage Mullitization in Temperature Range of 1200-1300 °C, *J. Eur. Ceram. Soc.*, 2005, **25**, p 613-626
20. C. Cano, E. Garcia, A.L. Fernandes, M.I. Osendi, and P. Miranzo, Mullite/ZrO_2 Coatings Produced by Flame Spraying, *J. Eur. Ceram. Soc.*, 2008, **28**(11), p 2191-2197
21. T. Höche, M. Deckwerth, and C. Rüssel, Partial Stabilization of Tetragonal Zirconia in Oxynitride Glass-Ceramics, *J. Am. Ceram. Soc.*, 1998, **81**(8), p 2029-2036
22. M. McCoy, W.E. Lee, and A.H. Heuer, Crystallization of MgO-Al_2O_3-SiO_2-ZrO_2 Glasses, *J. Am. Ceram. Soc.*, 1986, **69**(3), p 292-296
23. B.R. Marple, R.S. Lima, C. Moreau, S.E. Kruger, L. Xie, and M.R. Dorfman, Yttria-Stabilized Zirconia Thermal Barriers Sprayed Using N_2-H_2 and Ar-H_2 Plasmas: Influence of Processing and Heat Treatment on Coating Properties, *J. Therm. Spray Technol.*, 2007, **16**(5-6), p 791-797

Peer Reviewed